ACS APPLIED MATERIALS & INTERFACES

Research Article

www.acsami.org

Patterning of Gold Nanoparticles on Fluoropolymer Films by Using Patterned Surface Grafting and Layer-by-Layer Deposition Techniques

Chang-Hee Jung,[†,‡] In-Tae Hwang,[†] Chan-Hee Jung,*[,†] Jae-Hak Choi,*[,§] Oh-Sun Kwon,[‡] and Kwanwoo Shin[‡]

[†]Research Division for Industry and Environment, Advanced Radiation Technology Institute, Korea Atomic Energy Research Institute, Jeongeup-si, Jeollabuk-do 580-185, Republic of Korea

[‡]Department of Chemistry and Institute of Biological Interfaces, Sogang University, Mapo-gu, Seoul 121-742, Republic of Korea

[§]Department of Polymer Science and Engineering, Chungnam National University, Yuseong-gu, Daejeon 305-764, Republic of Korea

Supporting Information

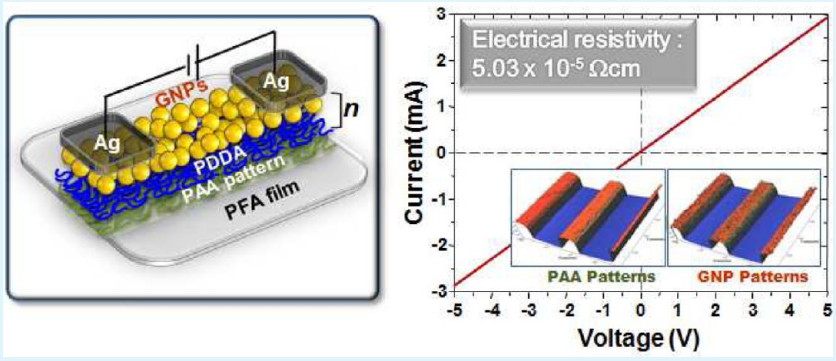

ABSTRACT: The patterning of gold nanoparticles (GNPs) on the surface of a fluoropolymer substrate by using patterned surface grafting and layer-by-layer deposition techniques is described. The surface of a poly(tetrafluoroethylene-co-perfluorovinyl ether) (PFA) substrate was selectively implanted with 150 keV proton ions. Peroxide groups were successfully formed on the implanted PFA surface, and their concentration depended on the fluence. Acrylic acid was graft polymerized onto the implanted regions of the PFA substrate, resulting in well-defined patterns of poly(acrylic acid) (PAA) on the PFA substrate. The surface properties of the PAA-patterned PFA surface, such as chemical compositions, wettability, and morphology, were investigated. The surface analysis results revealed that PAA was definitely present on the implanted regions of the PFA surface, and the degree of grafting was dependent on three factors: fluence, grafting time, and monomer concentration. Furthermore, GNP patterns were generated on the prepared PAA-patterned PFA surface by layer-by-layer deposition of GNPs and poly(diallyldimethyl ammonium chloride). The multilayers of GNPs were deposited only onto the PAA-grafted regions separated by bare PFA regions, and the resulting GNP patterns exhibited good electrical conductivity.

KEYWORDS: *ion implantation, poly(tetrafluoroethylene-co-perfluorovinyl ether), patterned surface grafting, poly(acrylic acid) patterns, layer-by-layer deposition, gold nanoparticles, electrical conductivity*

INTRODUCTION

Owing to the size-dependent properties of metal nanoparticles,[1−3] the fabrication of patterned metal nanoparticles has received a tremendous amount of attention for a variety of applications in biochemical, electronic, photonic, and magnetic devices.[4−6] Therefore, numerous studies on the patterning of metal nanoparticles using various techniques have been carried out on inorganic substrates such as glass, silicon, indium−tin oxide, and metal.[1]

The patterning of metal nanoparticles on polymer substrates has been of great interest over the past decade because polymer substrates are lightweight, flexible, and lower in cost.[7−9] Thus, a variety of synthetic polymers have been extensively explored as substrates for patterns of metal nanoparticles.[10−13] Among these polymers, fluoropolymers such as poly(tetrafluoroethylene-*co*-perfluorovinyl ether) (PFA), poly(tetrafluoroethylene) (PTFE), poly(tetrafluoroethylene-*co*-hexafluoropropylene) (FEP), and poly(vinylidene fluoride) (PVDF), have been considered suitable for metal patterning due to their high thermal stability, superior electric insulation, and excellent chemical resistance.[14−16] However, the use of these fluoropolymers has been limited in such applications due

Received: May 23, 2013
Accepted: August 8, 2013
Published: August 8, 2013

to their much lower surface energy in comparison to other synthetic polymers. Therefore, fluoropolymers should be subjected to surface modification for such applications.

Various physiochemical strategies including chemical oxidation treatment, plasma-enhanced chemical deposition coating, and surface grafting have been developed to modify the surface of polymer substrates.[17−19] Among them, surface grafting has attracted attention on account of its advantages over other techniques, such as the ability to tailor the surface energy and functionality to be appropriate for the next process, covalent attachment of surface functionality, and tunable incorporation of tethered chains onto the surface of a polymer substrate with high density while preserving their chemical nature.[20−22] Surface grafting has been performed by means of peroxide initiators, plasma-enhanced chemical deposition, and irradiation with UV-light, plasma, and ionizing radiation (ion and electron beams).[23−27] An ion impanation-induced surface grafting is an effective way to generate functional groups on the surface of a polymer substrate due to its reliability, controllability, effectiveness, and eco-friendly nature.[28−30] However, the surface modification of fluoropolymers by ion implantation-induced surface grafting has not been previously investigated to form patterns of metal nanoparticles.

Electrostatic layer-by-layer deposition is a convenient and powerful technique for the construction of multiple-layered metal nanoparticles on a curved substrate.[31−33] It is based on the sequential adsorption of complementary materials through electrostatic interaction, hydrogen bonding, and other complementary interactions. It is typically performed using sequential dip-coating of a substrate in positively and negatively charged material solutions.

In this study, the convenient and efficient patterning of gold nanoparticles (GNPs) on a fluoropolymer substrate through a combination of ion implantation-induced patterned surface grafting and layer-by-layer deposition was demonstrated, which can offer high conductivity without any additional thermal treatment steps. The surface modification of a fluoropolymer substrate by ion implantation-induced patterned surface grafting was investigated under various conditions to establish resolved functional patterns. Furthermore, the layer-by-layer deposition of GNPs on a selectively modified PFA substrate was performed to generate conductive GNP patterns.

EXPERIMENTAL SECTION

Materials. PFA films (250 μm thickness, Ashai Glass Co., Ltd.) were thoroughly washed in a ultrasonic cleaner (Branson Ultrasonic Corporation, 8510E-DTH) for 20 min and dried in a vacuum oven at 50 °C for 24 h before use. For surface grafting and characterization, acrylic acid, ammonium iron(II) sulfate hexahydrate ($(NH_4)_2Fe(SO_4)_2$, 99%), sulfuric acid (H_2SO_4, 98%), 1,1-diphenyl-2-picylhydrazyl (DPPH), and toluidine blue O supplied by Sigma-Aldrich were employed. For the synthesis of GNPs, hydrogen tetrachloroaurate (III) trihydrate ($HAuCl_4{\cdot}3H_2O$, >99.9%, Kojima Chemical Company) and trisodium citrate ($Na_3C_6H_5O_7{\cdot}2H_2O$, >99%, Sigma-Aldrich) were used. Poly(diallyldimethyl ammonium chloride) (PDDA, 20% in water, MW: 100,000−200,000, Sigma-Aldrich) was used as a positively charged polyelectrolyte. All chemicals were employed as received.

Preparation of PAA-Patterned PFA Substrates by Ion Implantation-Induced Patterned Surface Grafting. A 300 keV ion implanter installed at the Advanced Radiation Technology Institute (ARTI) of the Korea Atomic Energy Research Institute (KAERI) was utilized in the process of ion implantation. Well-cleaned PFA substrates were implanted with 150 keV proton ions at room temperature in the presence or absence of a pattern mask (SUS, 100 μm line and space). The fluence ranged from 5×10^{14} to 1×10^{16} ions/cm^2, and a current density lower than 1.0 μA/cm^2 was maintained to suppress an increase in the temperature of the samples. After the ion implantation, the resulting substrates were kept in air for 24 h.

For surface grafting, the implanted PFA substrates were immersed in an aqueous 5− 60 vol% acrylic acid solution containing 0.1 wt % $(NH_4)_2Fe(SO_4)_2$ and 0.2 M H_2SO_4 in glass vials, sealed with rubber septa, and finally purged with N_2 gas to eliminate the existing oxygen. $(NH_4)_2Fe(SO_4)_2$ and H_2SO_4 were utilized for the inhibition of homopolymerization and for the promotion of grafting, respectively. The vials were placed in a water bath at a constant temperature of 65 °C for 6−18 h. Afterward, the physically adsorbed homopolymers and monomers on the substrates were completely removed by water extraction. The resulting poly(acrylic acid) (PAA)-patterned PFA substrates were then dried in a vacuum oven at 50 °C at a residual pressure of 1×10^{-3} mbar for 24 h.

Layer-by-Layer Deposition of GNPs on PAA-Patterned PFA Substrates. Gold nanoparticles (GNPs) were prepared by the following procedure reported in the literature.[34] Briefly, a 1 mM $HAuCl_4{\cdot}3H_2O$ solution containing 0.012 g of $HAuCl_4{\cdot}3H_2O$ in 30 mL of distilled water was brought to a boil with continuous stirring, and subsequently 3 mL of 1 wt % aqueous trisodium citrate solution in distilled water was added. After the color change of the solution from dark gray to wine red, the reaction was stirred for an additional 15 min and then allowed to cool to room temperature. The mean diameters of the prepared GNPs were measured using a dynamic light scattering spectrometer (DLS, Otsuka Electronics, DLS-8000HL) and found to be around 14 nm (Figure S1,e Supporting Information).

GNP multilayers were formed on the PAA-patterned PFA substrates by a layer-by-layer deposition method reported in the literature.[35] Briefly, the prepared PFA substrates were immersed in a 2 wt % PDDA solution in distilled water. After incubation for 30 min, the resulting substrates were thoroughly washed with distilled water and dried with nitrogen gas. Next, the substrates were immersed in a freshly prepared GNP solution for 1 h, rinsed with distilled water, and then dried. This adsorption cycle of PDDA and GNPs was repeated from 1 to 14 times to form multilayered patterns of GNPs.

Characterization. The amount of peroxide groups generated on the PFA surface after ion implantation was measured using a well-known DPPH method as described in our previous work.[36] The grafting degree of the grafted PAA on the surface of the PFA substrates was measured using a toluidine blue O staining method as described in our previous works.[36−38] The chemical structure of the samples was investigated using an attenuated total reflectance Fourier transform infrared spectroscope (ATR-FT-IR, Varian 640, Australia) equipped with an ATR PIKE MIRacle accessory containing a ZnSe crystal. The chemical composition of the control, implanted, and PAA-grafted PFA surfaces was examined using an X-ray photoelectron spectrometer (MultiLab 2000, Thermoelectron Corporation, England) with a monochromatic Mg Kα source, and the Advantage 3.70 program was applied to deconvolute the C1s XPS spectra. The static contact angles of the control, implanted, and PAA-grafted PFA surfaces were measured using a Phoenix 300 contact angle analyzer (Surface Electro Optics Co., Ltd., Korea). The surface morphology, chemical composition, and profiles of the PAA-patterned PFA and multilayered GNP-deposited on the PAA-patterned PFA substrates were investigated using a field emission scanning electron microscope (FE-SEM, JEOL JSM-7500F) equipped with an energy dispersive X-ray spectrometer (EDX), a 3D optical surface profiler (NanoSystem), and an atomic force microscope (AFM, XE-100, Park System, Korea). To measure the current−voltage (I−V) characteristic of the GNP patterns on the PFA substrates, 250 μm wide silver electrodes were thermally deposited at both edges of the GNP patterns, and the average distance between them was about 8000 μm. The I−V curves were obtained using a probe station (MST-4000A) equipped with a Kiethley 2400 source meter.

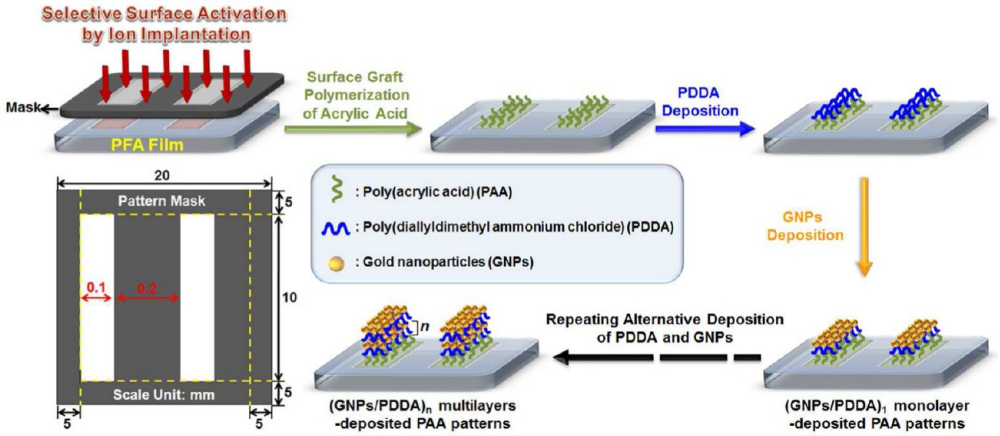

Figure 1. Schematic illustration of GNP patterning on a PFA substrate via ion implantation-induced patterned surface grafting and layer-by-layer deposition.

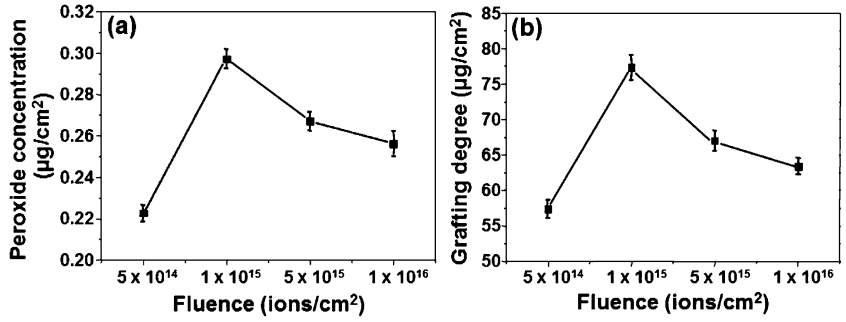

Figure 2. Peroxide concentration (a) and surface density of carboxylic acid groups (b) as a function of the fluence.

RESULTS AND DISCUSSION

Preparation of PAA-Patterned PFA Substrates by Ion Implantation-Induced Patterned Surface Grafting. Figure 1 shows a schematic illustration of GNP patterning on a PFA substrate through ion implantation-induced patterned surface grafting and layer-by-layer deposition. The surface of the PFA substrate was activated through implantation with accelerated proton ions in the presence of a pattern mask; thus, peroxide groups were selectively generated on the PFA surface that can be used as an initiator for surface grafting. Afterward, the surface grafting of acrylic acid was carried out on the selectively activated regions of the PFA surface at an elevated temperature to generate PAA patterns on the PFA substrate.[26,28,29] Finally, the layer-by-layer deposition of GNPs was carried out on the PAA-patterned PFA surface to form GNP patterns.

To investigate the optimal conditions for surface grafting, the surface grafting of acrylic acid on the PFA substrates was executed under various conditions of fluence, monomer concentration, and grafting reaction time. First, the peroxide concentrations of the implanted PFA surfaces at various fluences are shown in Figure 2a. The concentration of the formed peroxide groups was highest at the fluence of 1×10^{15} ions/cm^2. This result implies that peroxide groups were successfully formed on the implanted surface at lower fluences due to oxidation after ion implantation; however, at higher fluences over 1×10^{15} ions/cm^2, carbonization prevailed, resulting in a reduced peroxide concentration.[28,29,39]

Figure 2b shows the dependence of grafting degree on the fluence. The changes in the grafting degree in relation to fluence showed a similar tendency to that of peroxide concentration, as mentioned above. The highest grafting degree, 77.3 μg/cm^2, was obtained on the PFA implanted at a fluence of 1×10^{15} ions/cm^2, which exhibited the highest concentration of peroxide groups. This result can be attributed to the dependence of grafting degree on the peroxide concentration.[28,29,39]

Figure S2a of the Supporting Information shows the dependence of grafting degree on the concentration of acrylic acid. The grafting degree typically exhibited an increasing tendency as the acrylic acid concentration increased. The grafting degree increased to 89.5 μg/cm^2 with increasing concentration of acrylic acid. However, at a concentration of more than 40 vol%, the grafting was not well controlled, which resulted in an uneven PAA-grafted PFA substrate as presented in Figure S3 of the Supporting Information.

The change in the grafting degree with grafting reaction time is also shown in Figure S2b of the Supporting Information. The grafting degree initially increased with an increase in the reaction time and then leveled off with reaction times over 12 h. An explanation for this result can be given as follows.[29] As the reaction time increased to 12 h, the radical initiation for grafting brought about by the thermal decomposition of the formed peroxide groups on the implanted PFA surface prevailed, leading to an increase in the grafting degree. On the other hand, in the case of a reaction time of over 12 h, the grafting degree did not increase further owing to the depletion of all the peroxide groups formed on the PFA surface and the monomers for polymerization. On the basis of these results, the fluence, acrylic acid concentration, and reaction time for the optimal surface grafting in this study was 1×10^{15} ions/cm^2, 40 vol%, and 12 h, respectively.

ATR-FT-IR analysis was employed to investigate the chemical structure of the PFA surface after the implantation and surface grafting, and the results are presented in Figure 3.

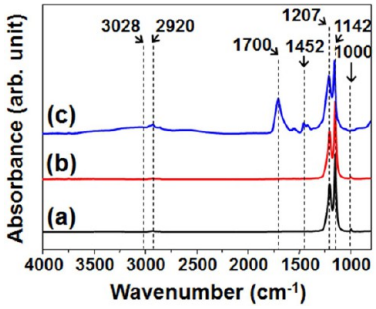

Figure 3. FTIR-ATR spectra of the control (a), implanted (b), and PAA-grafted PFA (c) films.

The PFA implanted at a fluence of 1×10^{15} ions/cm^2 and PAA-grafted PFA with a grafting degree of 77.3 μg/cm^2 were used for this analysis. As shown in Figure 3a, the characteristic peaks for the control PFA appeared at 1207 and 1142 cm^{-1} assigned to the stretching vibration of CF in the CF_2 group and at 1000 cm^{-1} assigned to the stretching vibration of CO in the alkoxy vinyl ether, respectively.[40] As shown in Figure 3b, the FT-IR spectrum of the implanted PFA was very similar to that of the control PFA. On the other hand, for the PAA-grafted PFA in Figure 3c, the main characteristic peaks for the COOH and CH_2 groups of the PAA were clearly observed at 3028, 2920, and 1700 cm^{-1}, respectively.[41] This result indicates that PAA was definitely present on the implanted PFA surface.

The chemical changes in the PFA surface caused by ion implantation and surface grafting were further investigated by an XPS analysis, and the results are shown in Figures S4 and S5 of the Supporting Information. Figure S4 of the Supporting Information represents the C1s core-level spectra of the control and implanted PFA substrates at the different fluences of 5×10^{14}, 1×10^{15}, 5×10^{15}, and 1×10^{16} ions/cm^2. The Cls spectrum of the control PFA substrate in Figure S4a of the Supporting Information shows the characteristic peaks at 293.2 (CF_3), 292.1 (CF_2), 286.5 (C−O), and 285.0 eV (C−C).[15,29] In the case of the implanted PFA substrates, new generation of the (C═O)−O peak and dramatic changes in the intensities of the existing peaks are shown in Figure S4b−e of the Supporting Information. These changes can be ascribed to the oxidation and defluorination induced by ion implantation. As shown in Figure S5b−e of the Supporting Information, in the case of the PAA-grafted PFA substrates, the chemical bonds existing in the spectra of the implanted PFA almost disappeared, and the characteristic peaks for the C−C and COOH of PAA were newly observed at 285, 286.5, and 289.1 eV.[15,29] In comparison to that of the implanted PFA, the intensity of CF_2 peaks was significantly reduced in the C1s spectra of the PAA-grafted PFA substrate prepared at the same fluence. Moreover, when compared to that of the implanted PFA at the same fluence, the [O]/[C] atomic ratio of the PAA-grafted PFA was remarkably elevated, whereas its [F]/[C] atomic ratio was noticeably reduced as shown in Figure 4. Accordingly, PAA was definitely present on the implanted PFA surface.

To clarify the influence of ion implantation and surface grafting on the wettability of the PFA, a water contact angle measurement was carried out (Figures S6, Supporting Information). Compared to the control PFA with a contact

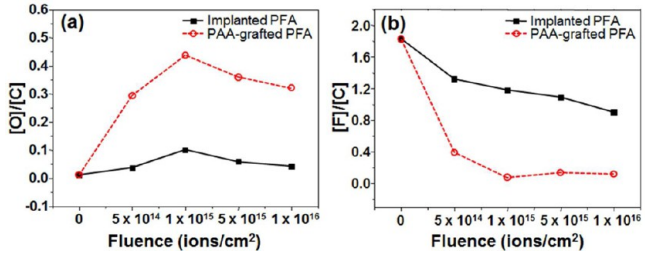

Figure 4. [O]/[C] and [F]/[C] ratios of the implanted (a) and PAA-grafted (b) PFA substrates obtained by XPS analysis as a function of the fluence.

angle of 105°, the contact angle of the implanted PFA was reduced to 86° with increasing fluence. In the case of the PAA-grafted PFA substrates, the contact angles were further reduced to 42° and depended on the grafting degree, which was higher than PAA with the contact angle of around 5°.[42] This result indicates that the effective ion implantation-induced surface grafting of hydrophilic acrylic acid brought about noticeable enhancement of the wettability of the PFA surface.

Figure 5 shows the FE-SEM image, 3D surface profile, and EDX spectrum of the PAA-patterned PFA substrate prepared

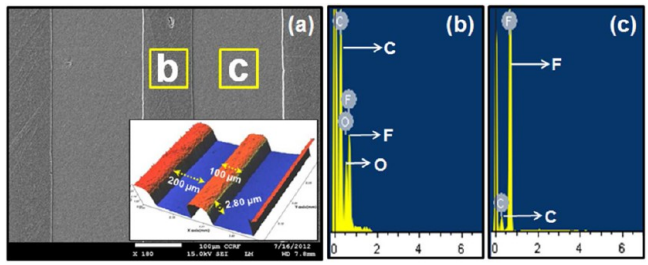

Figure 5. FE-SEM image of PAA-patterned PFA substrate and its corresponding EDX spectra ((b) and (c)) of the rectangles in (a). The inset of (a) shows 3D surface profile of the PAA-patterned PFA surface.

under optimized conditions. As shown in Figure 5a, well-defined 100 μm PAA patterns were clearly formed on the surface of a PFA substrate. As shown in the inset of Figure 5a, the thickness of the formed PAA patterns measured by a 3D optical surface profile analysis was 2.80 μm, and their width matched well with the results of the FE-SEM observation. Furthermore, as shown in Figure 5c, the EDX spectrum of the space region between the PAA-grafted regions exhibited only two elemental peaks corresponding to carbon (C) and fluorine (F) of the control PFA substrate, indicating that surface grafting did not occur on the nonimplanted regions. On the other hand, the EDX spectrum of the PAA-grafted regions in Figure 5b showed a new elemental peak for oxygen (O) in addition to the C and F peaks that are assigned to the characteristic elemental constituent of PAA. This result confirmed that PAA was present only on the implanted regions of the PFA surface. Thus, all of the PAA-patterned PFA substrates to further form GNP patterns through a layer-by-layer deposition were prepared under the above-mentioned optimized surface grafting condition.

Patterning of GNPs on the PFA Substrate by Layer-by-layer Deposition. The changes in the surface morphology of the PAA-patterned PFA substrate with the sequential layer-by-layer deposition of PDDA and GNPs were observed by FE-

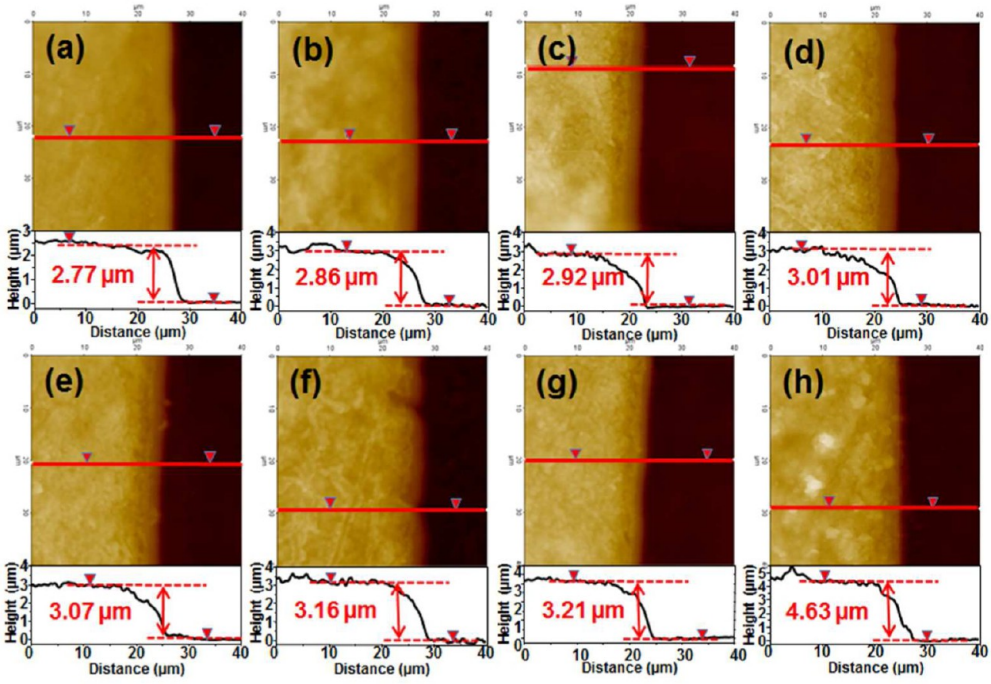

Figure 6. Contact mode AFM images and respective vertical distances in the height profile of the PAA-patterned PFA substrate (a), PDDA monolayer (b), $(GNPs/PDDA)_1$ (c), PDDA/$(GNPs/PDDA)_1$ (d), $(GNPs/PDDA)_2$ (e), PDDA/$(GNPs/PDDA)_2$ (f), $(GNPs/PDDA)_3$ (g), and $(GNPs/PDDA)_{14}$ layers (h) deposited on the PAA-patterned PFA substrate.

SEM, and the results are shown in Figure S7 of the Supporting Information. As shown in Figure S7b–h of the Supporting Information, all of the sequential layer-by-layer deposition of PDDA and GNPs successfully occurred only on the hydrophilic PAA regions separated by bare PFA regions by electrostatic interactions. As shown in the inset of Figure S7b of the Supporting Information, the surface of the PDDA-deposited PAA was much smoother than that of the original PAA. As shown in the inset of Figure S7c of the Supporting Information, the surface of the sequentially deposited GNPs and PDDA ($(GNPs/PDDA)_1$) on the PAA is much rougher than that of the PDDA-deposited PAA due to the introduction of spherical GNPs. As shown in the insets of Figure S7d–h of the Supporting Information, the deposited GNPs became denser with increasing numbers of GNPs and PDDA layers.

To further measure the thickness of the formed GNP multilayers on the PAA-patterned PFA substrate with sequential layer-by-layer deposition of PDDA and GNPs, an AFM analysis was carried out, and the results are shown in Figure 6. As shown in Figure 6b and c, the one-layer thickness of GNPs and PDDA ($(GNPs/PDDA)_1$) on the PAA was 150 nm, which approximately consisted of 60 nm thick GNPs and 90 nm thick PDDA layers. As shown in Figure 6d–g, in the case of more than two sequential layer-by-layer depositions of GNPs and PDDA, a 130 nm thickness of GNPs/PDDA was also equally deposited, which approximately consisted of a 50 nm thick GNP layer and an 80 nm thick PDDA layer. The difference in thickness between the initial layer and later layers of GNPs and PDDA could be ascribed to the fact that the presence of dense PAA in the patterns could generate the thicker deposition of the initial PDDA layer capable of the higher deposition of the GNPs in comparison to those of the later layers of GNPs and PDDA.[43,44] Therefore, the thickness of the 14 layers of GNPs and PDDA ($(GNPs/PDDA)_{14}$) was around 1860 nm.

To verify the formation of GNP patterns on the PFA substrate, the $(GNPs/PDDA)_{14}$ layer-deposited GNP patterns formed on PAA-patterned PFA substrate was analyzed by using FE-SEM equipped with EDA and 3D surface profiler (Figure 7). As shown in Figure 7a, well-defined 100 μm patterns of

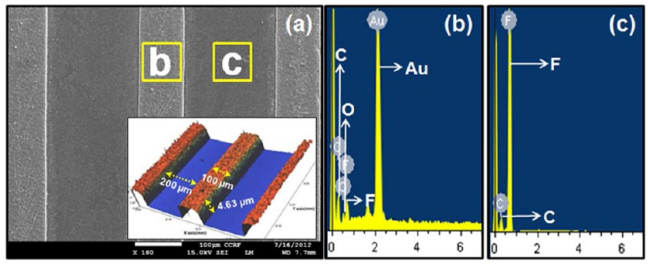

Figure 7. FE-SEM image of $(GNPs/PDDA)_{14}$-deposited PAA-patterned PFA substrate and its corresponding EDX spectra ((b) and (c)) of the rectangles in (a). The inset of (a) shows the 3D surface profile of the $(GNPs/PDDA)_{14}$ layers-deposited PAA patterns.

$(GNPs/PDDA)_{14}$ layer-deposited PAA were resolved on the PAA-patterned PFA substrate. As shown in the inset of Figure 7a, the thickness of the formed GNP patterns measured by a 3D optical surface profile analysis was 4.63 μm, and their width matched well with the results of the FE-SEM observation. In addition, as shown in Figure 7c, the EDX spectrum of the space regions between the GNP patterns exhibited two peaks for carbon (C) and fluorine (F) assigned to the elemental constituents of the PFA, indicating that the layer-by-layer deposition of GNPs and PDDA did not occur on the PAA-absent bare PFA regions. On the other hand, as shown in Figure 7b, two peaks for oxygen (O) and gold (Au) in addition to the C and F elements were newly identified in the EDX spectrum of the GNP patterns, indicating the occurrence of

dx.doi.org/10.1021/am4019687 | ACS Appl. Mater. Interfaces 2013, 5, 8546–8552

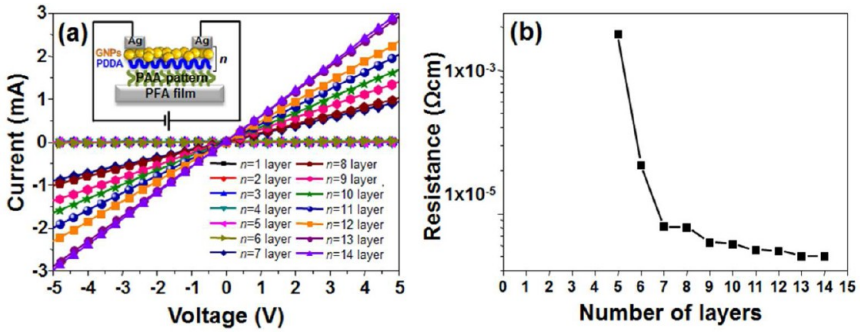

Figure 8. *I*−*V* curves (a) and electrical resistance obtained by the corresponding *I*−*V* curves (b) of the $(GNPs/PDDA)_n$-deposited PAA patterns on the PFA substrate with different layers (n).

layer-by-layer deposition of GNPs and PDDA on the PAA regions of the PAA-patterned PFA substrate. Therefore, the layer-by-layer deposition of GNPs and PDDA had successfully occurred only on the PAA regions separated by bare PFA regions, thus resulting in the formation of well-organized 100 μm GNP patterns.

To investigate the electronic properties of the GNP patterns with different layers of GNPs and PDDA ($(GNPs/PDDA)_n$), the *I*−*V* curves were recorded by applying a DC bias across the patterns with a top contact, and the results are presented in Figure 8. As shown in Figure 8a, all GNP patterns except the lower four layers of GNPs and PDDA ($(GNPs/PDDA)_{1-4}$) exhibited linear *I*−*V* behaviors, indicating the metallic property of the patterns and the ohmic contact between the GNP patterns and the Ag electrodes.[45,46] Furthermore, the electrical resistivity of the GNP patterns was calculated using the slope of the *I*−*V* curves, and the known dimensions of the respective GNP patterns, as presented in Scheme S1 of the Supporting Information. As shown in Figure 8b, the electrical resistivity of the GNP patterns was reduced to 5.03×10^{-5} Ω cm with increasing numbers of GNPs and PDDA layers. However, the electrical resistivity of the GNP patterns exhibited a saturation tendency above seven layers (Table S1, Supporting Information).

CONCLUSIONS

In this research, the patterning of GNPs on a PFA substrate via ion implantation-induced patterned surface grafting and layer-by-layer deposition was demonstrated. PAA-patterned PFA substrates were prepared by selective surface grafting of acrylic acid onto the implanted regions of the PFA surface. The fluence, monomer concentration, and reaction time for the optimal surface grafting in this study were 1×10^{15} ions/cm^2, 40 vol%, and 12 h, respectively. GNPs and PDDA were selectively deposited onto the PAA regions separated by bare PFA regions on the PAA-patterned PFA substrates, resulting well-organized 100 μm GNP patterns. On the basis of the *I*−*V* curves, the formed GNP patterns exhibited a linear *I*−*V* behavior, and their electrical resistivity was reduced to 5.03×10^{-5} Ω cm with increasing numbers of GNPs and PDDA layers. This technique can be applied to prepare patterned arrays of various metal nanoparticles, which are crucial for electrical and biological applications.

ASSOCIATED CONTENT

Supporting Information

Dynamic light scattering (DLS) profile of prepared GNPs; effect of acrylic acid concentration and grafting reaction time on the grafting degree; photographs of the PAA-grafted PFA films prepared at different monomer concentrations; Cls XPS spectra of the control, implanted, and PAA-grafted PFA substrates at different fluences; water contact angles of the control, implanted, and PAA-grafted PFA films at different fluences; FE-SEM images for the PAA-patterned PFA substrate after the sequential layer-by-layer deposition of PDDA and GNPs; graphic illustration for the resistivity calculation of $(GNPs/PDDA)_n$-deposited PAA patterns on the PFA substrate; and resistivity and conductivity of $(GNPs/PDDA)_n$-deposited PAA patterns on the PFA substrate with different layers (*n*). This material is available free of charge via the Internet at http://pubs.acs.org.

AUTHOR INFORMATION

Corresponding Author

*+82-42-821-6664. Fax: +82-42-821-8910. E-mail: jaehakchoi@cnu.ac.kr (J.-H.C.); jch@kaeri.re.kr (C.-H.J.).

Notes

The authors declare no competing financial interest.

ACKNOWLEDGMENTS

This work was supported by Radiation Technology R&D program through the National Research Foundation of Korea funded by the Ministry of Science, ICT, & Future Planning. K.S. acknowledges the financial support from the Mid-career Researcher Program (2011-0017539).

REFERENCES

(1) Shipway, A. N.; Katz, E.; Willner, I. *ChemPhysChem* **2000**, *1*, 18−52.
(2) Shipway, A. N.; Willner, I. *Chem. Commun.* **2001**, 2035−2045.
(3) Haryono, A.; Binder, W. H. *Small* **2006**, *2*, 600−611.
(4) Dirix, Y.; Bastiaansen, C.; Caseri, W.; Smith, P. *Adv. Mater.* **1999**, *11*, 223−227.
(5) Egusa, S.; Liau, Y. H.; Scherer, N. F. *Appl. Phys. Lett.* **2004**, *84*, 1257−1259.
(6) McFarland, A. D.; Young, M. A.; Dieringer, J. A.; Van Duyne, R. P. *J. Phys. Chem. B* **2005**, *109*, 11279−11285.
(7) Zschieschang, U.; Klauk, H.; Halik, M.; Schmid, G.; Dehm, C. *Adv. Mater.* **2003**, *15*, 1147−1151.
(8) Forrest, S. R. *Nature* **2004**, *428*, 911−918.
(9) Lee, H.; Hong, S.; Yang, K. *Appl. Phys. Lett.* **2006**, *88*, 143112.
(10) Won, J.; Ihn, K. J.; Kang, Y. S. *Langmuir* **2002**, *18*, 8246−8249.
(11) McAlpine, M. C.; Friedman, R. S.; Lieber, D. M. *Nano Lett.* **2003**, *3*, 443−445.
(12) Ko, S. H.; Pan, H.; Grigoropoulos, C. P.; Luscombe, C. K.; Frechet, J. M. J.; Poulikakos, D. *Nanotechnology* **2007**, *18*, 345202.

(13) Park, I.; Ko, S. H.; Pan, H.; Grigoropoulos, C. P.; Pisano, A. P.; Frechet, J. M. J.; Lee, E. S.; Jeong, J. H. *Adv. Mater.* **2008**, *20*, 489−496.
(14) Park, Y. W.; Inagaki, N. *Polymer* **2003**, *44*, 1569−1575.
(15) Okubo, M.; Tahara, M.; Sarki, N.; Yamamoto, T. *Thin Solid Films* **2008**, *516*, 6592−6597.
(16) Naujokas, A.; Abreu, D. G.; Takacs, G. A.; Debies, T.; Mehan, M.; Entenberg, A. *Surf. Interface Anal.* **2013**, *45*, 1056−1062.
(17) Kang, E. T.; Zhang, Y. *Adv. Mater.* **2000**, *12*, 1481−1494.
(18) Alf, M. E.; Asatekin, A.; Barr, M. C.; Baxamusa, S. H.; Chelawat, H.; Ozaydin-Ince, G.; Petruczok, C. D.; Sreenivasan, R.; Tenhaeff, W. E.; Trujillo, N. J.; Vaddiraju, S.; Gleason, K. K. *Adv. Mater.* **2010**, *22*, 1993−2027.
(19) Neuhaus, S.; Padeste, C.; Solak, H. H.; Spencer, N. D. *Polymer* **2010**, *51*, 4037−4043.
(20) Hu, S.; Ren, X.; Bachman, M.; Sims, C. E.; Li, G. P.; Allbritton, N. *Anal. Chem.* **2002**, *74*, 4117−4123.
(21) Edmondson, S.; Osborne, V. L.; Huck, W. T. S. *Chem. Soc. Rev.* **2004**, *33*, 14−22.
(22) Liu, N.; Sun, G.; Gaan, S.; Rupper, P. *J. Appl. Polym. Sci.* **2010**, *116*, 3629−3637.
(23) Deng, J.; Wang, L.; Liu, L.; Yang, W. *Prog. Polym. Sci.* **2009**, *34*, 156−193.
(24) Hu, S.; Brittain, W. J. *Macromolecules* **2005**, *38*, 6592−6597.
(25) Gupta, B.; Anjum, N. *Adv. Polym. Sci.* **2003**, *162*, 35−61.
(26) Dargaville, T. R.; George, G. A.; Hill, D. J. T.; Whittaker, A. K. *Prog. Polym. Sci.* **2003**, *28*, 1355−1376.
(27) Brack, H. P.; Padeste, C.; Slaski, M.; Alkan, S.; Solak, H. H. *J. Am. Chem. Soc.* **2004**, *126*, 1004−1005.
(28) Kim, D. K.; Choi, Y. M.; Jung, C. H.; Kwon, H. J.; Choi, J. H.; Nho, Y. C.; Suh, D. H. *Polym. Adv. Technol.* **2009**, *20*, 173−177.
(29) Choi, J. H.; Ganesan, R.; Kim, D. K.; Jung, C. H.; Hwang, I. T.; Nho, Y. C.; Yun, J. M.; Kim, J. B. *J. Polym. Sci., Part A: Polym. Chem.* **2009**, *47*, 6124−6134.
(30) Yun, J. M.; Jung, C. H.; Kim, D. K.; Hwang, I. T.; Choi, J. H.; Ganesan, R.; Kim, J. B. *J. Mater. Chem.* **2010**, *20*, 2007−2012.
(31) Decher, G. *Science* **1997**, *277*, 1232−1237.
(32) Chirea, M.; Garcia-Morales, V.; Manzanares, J. A.; Pereira, C.; Gulaboski, R.; Silva, F. *J. Phys. Chem. B* **2005**, *109*, 21808−21817.
(33) Ma, H.; Zhang, L.; Pan, Y.; Zhang, K.; Zhand, Y. *Electroanal.* **2008**, *20*, 1220−1226.
(34) Huang, H.; Yang, X. *Colloid. Surf., A* **2003**, *226*, 77−86.
(35) Ostrander, J. W.; Mamedov, A. A.; Kotov, N. A. *J. Am. Chem. Soc.* **2001**, *123*, 1101−1110.
(36) Jung, C. H.; Hwang, I. T.; Kuk, I. S.; Choi, J. H.; Oh, B. K.; Lee, Y. M. *ACS Appl. Mater. Interfaces* **2013**, *5*, 2155−2160.
(37) Sano, S.; Kato, K.; Ikada, Y. *Biomaterials* **1993**, *14*, 817−822.
(38) Ying, L.; Yin, C.; Zhuo, R. X.; Leong, K. W.; Mao, H. Q.; Kang, E. T.; Neoh, K. G. *Biomacromolecules* **2003**, *4*, 157−165.
(39) Zang, Y.; Huan, A. C. H; Tan, K. L.; Kang, E. T. *Nucl. Instrum. Methods Phys. Res., Sect. B* **2000**, *168*, 29−39.
(40) Nasef, M. M. *Polym. Int.* **2001**, *50*, 338−346.
(41) El Sawy, N. M. *Polym. Int.* **2004**, *53*, 212−217.
(42) Wouters, D.; Van Camp, W.; Dervaux, B.; Du Prez, F. E.; Schubert, U. S. *Soft Matter* **2007**, *3*, 1537−1541.
(43) Yoo, D.; Shiratori, S. S.; Rubner, M. F. *Macromolecules* **1998**, *31*, 4309−4318.
(44) Glinel, K.; Moussa, A.; Jonas, A. M.; Laschewsky, A. *Langmuir* **2002**, *18*, 1408−1412.
(45) Du, R.; Ssenyange, S.; Aktary, M.; McDermott, M. T. *Small* **2009**, *5*, 1162.
(46) Zhang, Y.; Guo, L.; Wei, S.; He, Y.; Xia, H.; Chen, Q.; Sun, H. B.; Xiao, F. S. *Nano Today* **2010**, *5*, 15−20.